

# Characterization of Trimetallic Pt-Pd-Au/CeO<sub>2</sub> Catalysts Combinatorial Designed for Methane Total Oxidation

András Tompos<sup>a</sup>, József L. Margitfalvi<sup>\*a</sup>, Mihály Hegedűs<sup>a</sup>, Ágnes Szegedi<sup>a</sup>, Jose Luis G. Fierro<sup>b</sup> and Sergio Rojas<sup>b</sup>

<sup>a</sup>*Institute of Surface Chemistry and Catalysis, Chemical Research Center, Hungarian Academy of Sciences, 1525 Budapest, P.O. Box 17, Hungary*

<sup>b</sup>*CSIC, Inst. Catalis and Petroleoquim, Madrid, E-28049, Spain*

**Abstract:** In the present work, the role and the effect of platinum and gold on the catalytic performance of ceria supported tri-metallic Pt-Pd-Au catalysts have been studied. The optimum composition of these tri-metallic supported catalysts has been discovered using methods and tools of combinatorial catalyst library design. Detailed catalytic, spectroscopic and physico-chemical characterization of catalysts in the vicinity of the optimum in the given compositional space has been performed. The temperature-programmed oxidation of methane revealed that the addition of Pt and Au to Pd/CeO<sub>2</sub> catalyst resulted in higher conversion values in the whole investigated temperature range compared to the monometallic Pd catalyst. The time-on-stream experiments provided further evidence for the high-stability of tri-metallic catalysts compared to the monometallic one. Kinetic studies revealed the stronger adsorption of methane on Pt-Pd/CeO<sub>2</sub> catalysts than over Pd/CeO<sub>2</sub>. XPS analysis showed that Pt and Au stabilize Pd in a more reduced form even under condition of methane oxidation. FTIR spectroscopy of adsorbed CO and hydrogen TPD measurements provided indirect evidences for alloying of Pt and Au with Pd. CO chemisorption data indicated that tri-metallic catalysts have increased accessible metallic surface area. It is suggested that advantageous catalytic properties of tri-metallic Pt-Au-Pd/CeO<sub>2</sub> catalysts compared to the monometallic one can be attributed to (i) suppression of the formation of ionic forms of Pd(II), (ii) reaching an optimum ratio between Pd<sup>0</sup> and PdO species, and (iii) stabilization of Pd in high dispersion. The results also indicate that Pd<sup>0</sup> – PdO ensemble sites are required for methane activation.

**Keywords:** Combinatorial catalysis, FTIR, high throughput experimentation, methane oxidation, Pd<sup>0</sup>-PdO ensemble sites, Pt-Au-Pd catalysts, tri-metallic catalysts, XPS.

## INTRODUCTION

Abatement of methane emission from natural gas vehicles is one of the most important and challenging issues of environmental protection. Contribution of methane to the global warming is much higher than that of carbon dioxide; moreover its lifetime is quite long. As compared to other hydrocarbons the total oxidation of methane is more difficult because of its higher stability. This is the reason why many authors have chosen methane as a model compound for catalytic oxidation studies, assuming that total oxidation of other hydrocarbons would be guaranteed if methane was quantitatively abated.

The complete oxidation of methane can be performed over either noble metals or transition metal oxides. The main advantage of noble metals is their superior specific activity, which makes them as the best candidates for low temperature combustion of hydrocarbons. Supported Pd catalysts have been widely studied in methane catalytic oxidation [1-10]. However, the monometallic Pd catalysts have not proven to be appropriate for practical use because of significant activity loss in time-on-stream tests.

In order to understand the catalytic behavior of Pd based catalysts the nature of active sites was extensively studied in the PdO/Pd systems [3-7]. Common redox mechanism is confirmed in which Pd-PdO dual site is suggested to be active species. According to this mechanism Pd is involved in the activation of methane. The activated surface complex or the fragments (H and CH<sub>x</sub> (x = 3–1)) reduce the PdO to Pd, which is then reoxidized to PdO [5,6]. The ratio of PdO to Pd in the catalyst has to be optimized for obtaining the optimum catalytic performance [6]. Additionally, in another study the formation of two different types of PdO ((I) and (II)) with different activity in methane combustion has been proposed [7]. It has been suggested that in (I) the boundary contact between PdO and metallic Pd is responsible for the high activity of methane combustion. As the temperature increases the PdO (I) species are supposed to be transformed into PdO (II) that has low activity. In other study it has been shown that the deactivation of monometallic Pd catalysts can also be attributed to sintering [8] and poisoning [9,10] effects.

In order to improve and stabilize the activity of Pd catalysts it is advisable to modify the support or the active phase by addition of metals and/or other additives, i.e. to prepare multi-component palladium catalysts. However, in case of methane total oxidation only few studies have been devoted to the investigation of supported Pd-based bimetallic catalysts. The improved stability of supported Pd-Pt catalysts has

\*Address correspondence to this author at the Institute of Surface Chemistry and Catalysis, Chemical Research Center, Hungarian Academy of Sciences, 1525 Budapest, P.O. Box 17, Hungary; Tel: +36-1-3257747; Fax: +36-1-3257554; E-mail: joemarg@chemres.hu

been attributed to increased resistance towards sintering of Pd-Pt particles compared to Pd [11]. In this respect, it has to be emphasized that supported monometallic platinum catalyst is not really active for low temperature methane oxidation. This observation has been confirmed by earlier combinatorial study [12]. Consequently, the increased activity of Pd-Pt bimetallic catalysts cannot be attributed to the increased overall metal content, but to alteration of the structure of the active Pd sites. The results showed that the bimetallic catalyst has better time-on-stream activity during steady state operation as compared to the monometallic palladium catalyst. In addition, it has to be emphasized that the activity of the bimetallic catalyst was slightly higher than that of the monometallic palladium one.

Janbey *et al.* reported that the high activities observed over the bimetallic catalysts are due to the fact that they remain, at least partly, in the metallic state even under condition of methane oxidation [13]. The authors found higher activity and paradoxically higher activation energies for bimetallic catalysts in comparison to the monometallic Pd catalyst. The high activation energy indicates the presence of metallic palladium in the working catalyst [13].

In our recent study, we applied methods and tools of combinatorial catalysis and high throughput experimentation for the optimization of supported metal catalysts for methane oxidation [12]. This kind of approach is often used when the performance of a single component supported metal catalyst has to be improved. For catalysts used in total oxidation of methane, the following differentiation was done between the components of an active catalyst: (i), active metals; (ii), promoters of the active metals; (iii), new type of supports; and (iv), modifiers of the support. The best 15 catalysts designed by combinatorial methods contained mostly Ce and a small amount of La as a modifier in the support, while Pd, Pt and Au in small amount represented the active metallic phase [12]. It has to be emphasized that in the course of finding the optimized catalyst compositions no attempt was done to characterize the catalysts prepared. In the process of optimization all reaction parameters such as reaction temperature and space velocity were fixed and only the composition of catalysts was altered according to the optimization algorithm used [12]. According to research strategy accepted in combinatorial catalysis kinetic studies, physical-chemical and spectroscopic characterizations are performed only on series of optimized catalysts, but not over the whole catalyst library.

The main goal of the present study is to perform detailed investigation and elucidation of the effects of the addition of Pt and Au on the performance of ceria supported Pd catalyst. In this study the monometallic Pd/CeO<sub>2</sub> will be considered as a reference catalyst. An additional aim of this work is the demonstration that high-throughput hardware (parallel multi-reactors for both the preparation and testing of catalysts) can be used not only for optimization tasks but also for comparative studies of different catalysts, i.e. high throughput methods can also be used as a tool in academic, basic research.

## EXPERIMENTAL

### Preparation of Catalysts

The catalytic materials were prepared parallel by means of a liquid dispensing robot in Syncore reactor (BÜCHI La-

bortechnik AG, Switzerland) using the rack for 24 glass reaction vessels. The following precursor compounds were used for catalyst preparation: (NH<sub>4</sub>)<sub>2</sub>Ce(NO<sub>3</sub>)<sub>6</sub> (Fluka, >99.0%), Pt(NH<sub>3</sub>)<sub>4</sub>(NO<sub>3</sub>)<sub>2</sub> (Aldrich, 99.99%), Pd(NO<sub>3</sub>)<sub>2</sub>\*2H<sub>2</sub>O (Fluka, >98.0%) and HAuCl<sub>4</sub>\*3H<sub>2</sub>O (Aldrich, 99.99%).

As a first step CeO<sub>2</sub> support was prepared by means of urea precipitation technique applied in our previous study [12]. Water solution of the precursor (0.5 M) was dispensed and then 15 ml 2 M urea solution was added in water. In the Syncore reactor the solutions were heated upto to 100 °C and continuously shaken at 350 rpm. The resulting gels were vigorously boiled for 8 h at 100 °C to remove excess urea and to age the gels. After aging the precipitates were filtered and washed twice in deionized water and dried at 100 °C. Dried and milled samples were calcined in air at 400 °C for 2 h. The heating rate was 10 °C/min. BET specific surface area of CeO<sub>2</sub> prepared was 167 m<sup>2</sup>/g in this way.

In the second step 200 mg of the supports prepared as above was loaded with Pt and Pd using impregnation method. Precursor solutions (0.01 M in water) in the required amount were premixed and then the support was added. Water was evaporated at 100 °C under constant shaking at 350 rpm. The samples were dried at 100 °C and calcined again at 400 °C for 2 h (10 °C/min). In this way catalysts with different Pt content were prepared. The Pt content varied from 0 to 2.2 w/w% in increments of 0.2 w/w% resulting in 12 different catalysts. The Pd content of these Pt-Pd/CeO<sub>2</sub> catalysts was constant at 3 w/w%.

In the last step of the preparation gold was added using the urea precipitation method again. Diluted solution of gold precursor (0.01 M) was mixed with 5 ml 2 M urea then the dried and calcined Pt-Pd/CeO<sub>2</sub> catalyst, obtained in the previous preparation step, was added. The slurries were gradually heated upto 100 °C and this temperature was maintained for 4 h. The filtered samples were finally dried at 100 °C and calcined at 400 °C for 2 h (10 °C/min). In this way the catalyst containing 2 w/w% Pt and 3 w/w% Pd has been modified by 0.4 w/w% Au. Catalysts prepared in this way and not treated further will be called "as prepared" catalysts.

### Catalytic Tests

For catalytic test a 16-channel flow-through reactor was used at atmospheric pressure [12,14]. Prior to the activity tests the catalysts have been pressed, crushed and sieved. Catalysts with particle size between 0.200-0.315 mm were used in activity tests. 100 mg catalyst was placed into each reactor channel. Prior to the reaction the catalysts were pre-treated in H<sub>2</sub> (30 ml/min/channel) at 350 °C for 1 h, then the reactor was cooled to the reaction temperature in flowing He (30 mL/min/channel).

During temperature programmed oxidation (TPO) a gaseous mixture containing 1% CH<sub>4</sub>, 10% O<sub>2</sub> and 89% He was fed at the rate of 10 mL/min/channel. The reaction temperature was controlled between 150-400 °C with a heating rate 1 °C/min. Kinetic studies were performed in order to determine the reaction order of methane in the combustion reaction. In these experiments the reaction temperature was 280 °C and the total flow rate varied between 10 and 50 ml/min/channel. It has to be mentioned that at this temperature the reaction was kinetically controlled on all of the cata-

lysts investigated. Comparing results using 50 and 100 mg catalyst no mass transfer limitation was found over a supported catalyst containing 1 wt% Pt and 2 wt% Pd on pure CeO<sub>2</sub>. The initial reaction rates were calculated from the conversion – contact time dependencies, from which the reaction order for methane was determined.

The 16 outgoing reaction mixtures were analyzed consecutively by means of a quadrupole mass spectrometer (Prisma QMS 200). The conversion was determined by measuring the intensity of mass fragment of  $m/z$  15 characteristic for methane. In the first channel the catalyst was replaced by pure quartz. This channel was used for blank experiment with conversion equal to zero. The methane conversion for a given channel,  $\alpha_{\text{CH}_4}^{\text{ch}}$ , has been calculated according to the following equation:

$$\alpha_{\text{CH}_4}^{\text{ch}} = \frac{(I_{\text{CH}_4}^{\text{blank}} - I_{\text{CH}_4}^{\text{back}}) - (I_{\text{CH}_4}^{\text{ch}} - I_{\text{CH}_4}^{\text{back}})}{I_{\text{CH}_4}^{\text{blank}} - I_{\text{CH}_4}^{\text{back}}} \cdot 100, \% \quad (1)$$

where  $I_{\text{CH}_4}^{\text{blank}}$  and  $I_{\text{CH}_4}^{\text{ch}}$  are the intensities of the methane peak (fragment  $m/z$  15) in the blank channel and the selected channel, respectively.  $I_{\text{CH}_4}^{\text{back}}$  is the background intensity for  $m/z$  15. This is measured, in each channel, in the absence of methane feed. This signal is independent of methane conversion.

Considering the detection error in mass spectrometric analysis and the error propagation law the absolute error of conversion has been calculated to be +/- 0.4%. The fragment ion of  $m/z$  28 was monitored in order to check the formation of CO. Only CO<sub>2</sub> and water were detected as reaction products, which were verified by mass balance calculations. The entire apparatus is PC controlled using Xmea for Linux, our process control and data acquisition software.

### X-Ray Photoelectron Spectroscopy Analysis

X-ray photoelectron spectroscopy (XPS) studies were conducted on a VG Escalab 200 R spectrometer equipped with a hemispherical electron analyzer and an Mg-K $\alpha$  (1253.6 eV) X-ray source. The XP spectrometer was equipped with a chamber for sample treatment under controlled gas atmospheres and at temperatures upto 700 °C. A certain region of the XP spectrum was scanned a number of times to obtain a good signal-to-noise ratio. The binding energies (BEs) were referenced to the well-resolved peak (916.5 eV) in the Ce 3d core level region to account for charging effects.

Spectra of the as prepared samples as well as spectra after two different pretreatments performed in the pretreatment chamber of the spectrometer were recorded. After each pretreatment the samples were degassed at room temperature. First, the as prepared samples were analyzed without any treatment. In the subsequent pretreatment, the samples were reduced in a hydrogen atmosphere at 350 °C, while in the second pretreatment the samples were exposed to the reaction mixture applied in the catalytic runs (1% CH<sub>4</sub>, 10% O<sub>2</sub> and 89% He, at 350 °C for one hour). Spectra were processed by means of XPSPEAK software. The areas of the peaks were computed by fitting the experimental spectra to Gaus-

sian/Lorentzian curves after removing the background using the Shirley function.

### Fourier Transformed Infrared Spectroscopy of Adsorbed CO

*In situ* infrared spectra were recorded at room temperature using Nicolet Impact 400 FTIR instrument. The spectral region and the resolution were 3500–1100 cm<sup>-1</sup> and 1 cm<sup>-1</sup>, respectively. Catalyst samples were ground, pressed onto self-supporting disks and were mounted in the sample holder. The weight of the self-supporting disks was about 10–15 mg/cm<sup>2</sup>. The spectra were corrected for the weight of the sample. The thermal treatment of the sample was accomplished in a heated attachment chamber located above the IR cell. The catalysts were reduced in flowing hydrogen (50 ml/min) at 400 °C for 1 h followed by evacuation at the same temperature for 15 min and cooling to room temperature under vacuum. FTIR spectra were measured under static condition at P<sub>CO</sub> = 5 mbar. Spectra were obtained after accumulation of 128 scans. First the background spectra were measured, followed by the introduction of CO and spectra were taken after 30 min. Finally, the chamber was evacuated and spectra were taken after 30 min.

### Temperature Programmed Desorption of Hydrogen

For temperature programmed desorption (TPD) of hydrogen the ASDI RXM 100 equipment (Advanced Scientific Designs, Inc.) was applied. 50 mg of catalyst was loaded in a U shaped quartz reactor. Samples were pretreated at 350 °C (heating rate: 10 °C/min) in hydrogen flow (50 mL/min) for 1.5 h and then cooled to RT in hydrogen within 2 h. The gas flow (50 ml/min) was then switched to pure Ar. In a TPD run the temperature was raised from RT to 800 °C (heating rate: 10 °C/min), while the hydrogen desorption was followed by a TCD detector.

### Chemisorption of CO

The ASDI RXM 100 equipment was also used for CO chemisorption measurements. Because oxygen from ceria can react with CO adsorbed on Pd at near room temperature [15] and because CO<sub>2</sub> can adsorb on reduced ceria [15, 16] a fixed pretreatment procedure similar as described in ref. [17] was used on each catalyst. 50 mg of a given catalyst sample was loaded into a U shaped quartz reactor. The sample was heated under Ar flow (50 mL/min) to 150 °C (10 °C/min) and this temperature was maintained for 30 min. The sample was then reduced in a gas flow (200 Torr H<sub>2</sub> in Ar) for 1.5 h at 350 °C to transform Pd to its metallic form. Finally, the sample was purged with Ar (50 mL/min) at 350 °C and cooled to room temperature. Irreversible CO chemisorption was determined as a difference of total and reversible CO uptakes in the range of 0–20 Torr. Irreversible CO chemisorption is considered linearly proportional with the accessible metallic area.

## RESULTS AND DISCUSSION

### Catalytic Measurements in 16-Channel Flow-Through Reactor

In order to reveal the effect of the addition of Pt to the monometallic Pd/CeO<sub>2</sub> catalyst, twelve bimetallic catalysts

with different Pt content and constant Pd load have been prepared and tested as described in the experimental part. According to catalyst library optimization results small amount of gold (0.1-0.4 wt%) was also required to achieve the optimum high activity, however, too much gold had a definite negative effect on the methane conversion [12]. Therefore, in the present study a catalyst with 0.4 wt% Au content has also been prepared and investigated.

### Temperature Programmed Oxidation of Methane

Fig. 1 shows results of temperature-programmed oxidation of methane on a few selected catalysts. As emerges from Fig. 1 the methane conversion values measured on all multi-metallic catalysts exceed that of obtained on monometallic Pd catalyst in the whole investigated temperature range. Over multi-metallic catalysts the reaction temperatures that correspond to the 50 and 90% conversion values ( $T_{50}$  and

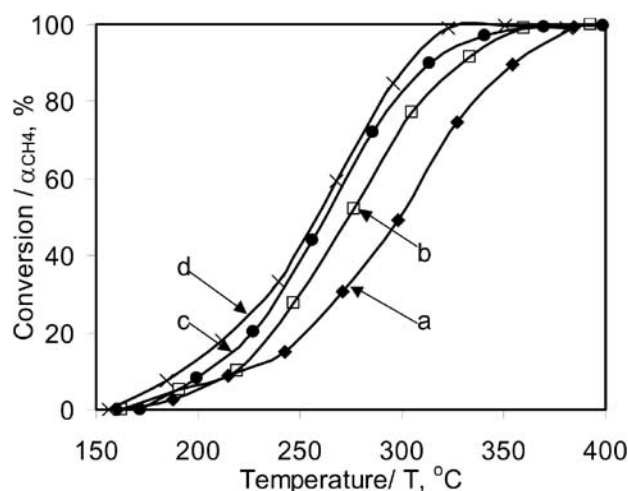


**Fig. (1).** Thermal programmed oxidation (TPO) of methane over catalyst; (a) 3%Pd/CeO<sub>2</sub>, (b) 1%Pt-3%Pd/CeO<sub>2</sub>, (c) 2%Pt-3%Pd/CeO<sub>2</sub>, (d) 2%Pt-3%Pd-0.4%Au/CeO<sub>2</sub>. Loading: 100 mg catalyst; feed: 1% CH<sub>4</sub>, 10% O<sub>2</sub> and 89% He; flow rate: 10 mL/min; heating rate: 1 °C/min.

$T_{90}$  values, respectively) are generally less than the corresponding data obtained on the monometallic Pd catalyst (Table 1). It can be concluded that the addition of both Pt and Au to Pd had a strong positive effect in the activity control.

**Table 1. Results of Temperature Programmed Oxidation of Methane**

Catalysts	$T_{50}^{**}$	$T_{90}^{**}$
	°C	°C
3%Pd/CeO <sub>2</sub> <sup>*</sup>	299	354
1%Pt-3%Pd/CeO <sub>2</sub>	263	312
2%Pt-3%Pd/CeO <sub>2</sub>	257	307
2%Pt-3%Pd-0.4%Au/CeO <sub>2</sub>	252	302

\*reference catalyst.

\*\* $T_{50}$  and  $T_{90}$  indicate reaction temperatures at which the conversion is 50 and 90%, respectively.

Further results are given in Fig. 2, where the corresponding  $T_{50}$  and  $T_{90}$  values are plotted as a function of Pt/Pd ratio. The addition of small amount of Pt to Pd already resulted in a significant drop in both  $T_{50}$  and  $T_{90}$  values as it is clearly evidenced from Fig. 2. Presumably, the results show that upon addition of platinum to Pd new type of active sites are forming.

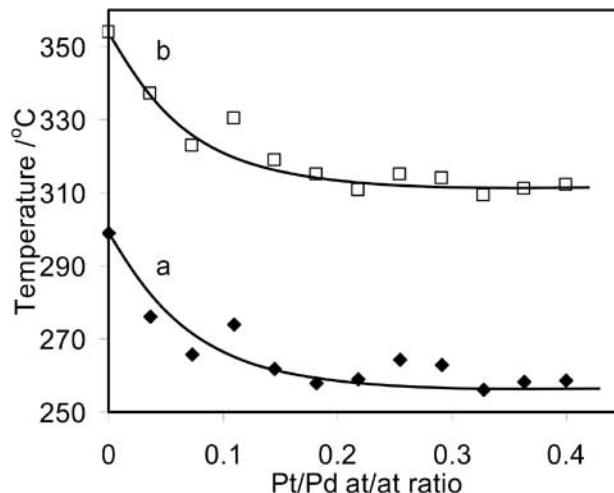


**Fig. (2).** Effect of Pt content on  $T_{50}$  (a) and  $T_{90}$  (b) values of different catalysts in TPO runs. Loading: 100 mg catalyst; feed: 1% CH<sub>4</sub>, 10% O<sub>2</sub> and 89% He; flow rate: 10 mL/min; heating rate: 1 °C/min.  $T_{50}$  and  $T_{90}$  indicate reaction temperatures at which the conversion is 50 and 90%, respectively.

The analysis of TPO curves given in Fig. 1 clearly shows the differences in the slope of the steepest section of the conversion-temperature dependencies. In the case of monometallic Pd catalyst the increase of conversion ( $\alpha$ ) with temperature is quite slow, i.e. the  $(\Delta\alpha/\Delta T)_{\max}$  values are relatively low. Contrary to that over all multi-metallic catalysts the  $(\Delta\alpha/\Delta T)_{\max}$  values are much higher. This fact indicates that all multi-metallic catalysts have higher activity, which is, however, paradoxically associated with higher activation energy. This observation is in a good accordance with results published by Janbey *et al.* [13]. Moreover, in an earlier study [3] it has been mentioned that the metallic Pd has significantly higher activity in methane oxidation than PdO, although the apparent activation energy over oxidized PdO catalyst was much lower than over metallic Pd (65-75 kJ/mol and 165-185 kJ/mol, respectively). Because of the higher activation energies and higher activity of the bimetallic systems it was suggested that in these catalysts the Pd phase must be, at least partly, in metallic state [13]. Therefore, the coexistence of both metallic Pd and oxidized PdO species is supposed to be present in our bimetallic Pt-Pd/CeO<sub>2</sub> catalysts, which may constitute a new type of active site for methane oxidation.

### Stability Tests

Fig. 3 shows the time-on-stream (TOS) activity pattern in methane oxidation at 280 °C on both monometallic and a bimetallic catalysts (2% Pt-3% Pd). Higher activity and slower rate of deactivation can be observed on the bimetallic catalyst containing 2% Pt and 3% Pd compared to the monometallic Pd catalyst. The rates of deactivation are ex-

pressed as  $\Delta\alpha/\alpha_{\text{ini}}$  (where  $\Delta\alpha$  is the conversion change measured after 350 min with respect to the initial conversion, while  $\alpha_{\text{ini}}$  is the initial conversion measured after 15 min).

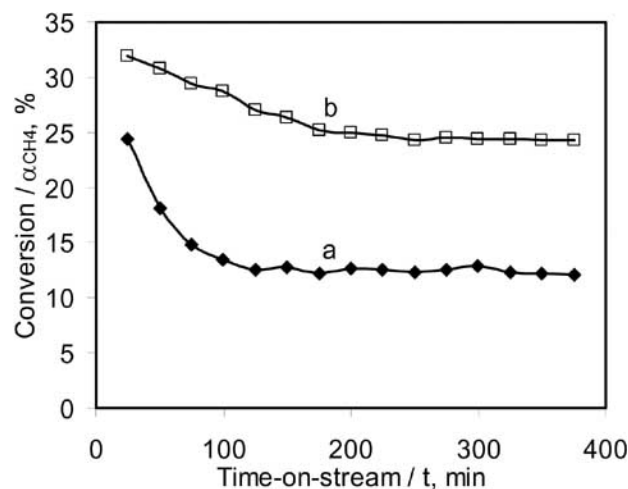


**Fig. (3).** Time-on-stream studies on catalysts; (a) 3%Pd/CeO<sub>2</sub> and (b) 2%Pt-3%Pd/CeO<sub>2</sub>. Loading: 100 mg catalyst; feed: 1% CH<sub>4</sub>, 10% O<sub>2</sub> and 89% He; flow rate: 50 mL/min; temperature: 280 °C.

The rates of deactivation measured over bimetallic catalysts with different Pt content are summarized in Table 2. As emerges from data given in Table 2 with increasing Pt content the  $\Delta\alpha/\alpha_{\text{ini}}$  ratio significantly decreases. The monometallic Pd catalyst loses almost half of its initial activity, while over the bimetallic catalyst containing 2% Pt only 24% loss of conversion was obtained.

It has to be emphasized that before the reaction the catalysts have been pretreated at 350 °C in hydrogen. Therefore, it is highly probable that all components are in metallic form or at least they are more reduced than during the catalytic reaction in the presence of an oxidative atmosphere. In TOS measurements under lean conditions applied in this study the oxidative atmosphere can result in the oxidation of both Pt and Pd. In an earlier study the formation of two different types of PdO has been proposed [7], one is active and other is inactive in methane oxidation. It is not excluded that the role of Pt, in this case, is to stabilize PdO in its more active form. According to the results presented in the above study the differences in the rates of formation of these two oxidized forms of Pd in different catalysts might account for the altered TOS activity of these catalysts. Literature data also indicate that sintering induced by the oxidative atmosphere can also be responsible for catalyst deactivation [8].

### Kinetic Studies

Kinetic studies were performed in order to determine the reaction order of methane in the oxidation reaction. The

measurements were done at 280 °C. The TPO curves (Fig. 1) clearly indicated that at this temperature the reaction was kinetically controlled over all catalysts. At this temperature the slope of the temperature – conversion dependencies is relatively high (Fig. 1), which indicates that the reaction rate is determined by the activation energy and not by diffusion limitations.

In this series of experiments the concentration of the methane was changed in the reaction mixture, then initial reaction rates were determined from the kinetic curves (conversion – contact time dependencies) obtained, from which the reaction order of methane was calculated. As emerges from Fig. 4, similarly to T<sub>90</sub> data, the presence of small amount of Pt leads to sudden drop in the reaction order, while above Pt/Pd > 0.25 the reaction order is constant.

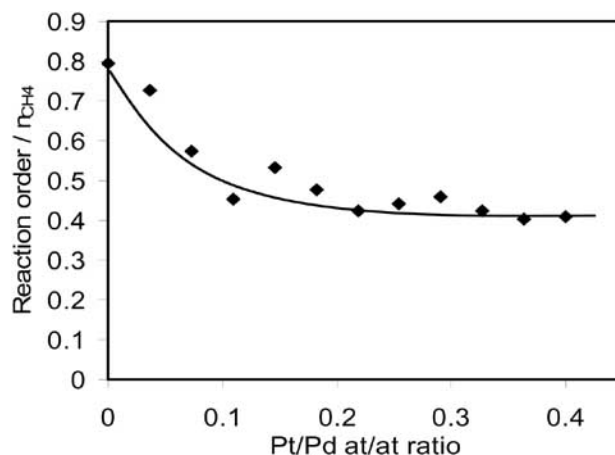


**Fig. (4).** Effect of Pt content on reaction order of methane. Loading: 100 mg catalyst; feed: 1-4% CH<sub>4</sub>, 10% O<sub>2</sub>, He balance; flow rate: 10-50 mL/min; temperature: 280 °C.

In case of competitive adsorption of two reactive species on the same type of active site the decrease in the reaction order always indicates an increase in the strength of adsorption of the molecule. Therefore, we consider that upon introduction of Pt the formation of new type of active site takes place, which regardless to the oxidation state of its components provides stronger adsorption site for methane, which can be one of the reasons for the higher activity over multi-metallic catalysts.

### X-Ray Photoelectron Spectroscopy Analysis

XP spectra obtained on catalyst containing all three noble metals (2%Pt-3%Pd-0.4%Au/CeO<sub>2</sub>) are given in Fig. 5. These figures show the binding energies of Pd, Pt, Au and Ce species, respectively after different pretreatment procedures. In this study the following treatment processes were applied: (a) calcination at 400 °C (*as prepared catalysts*), (b)

**Table 2.** Rate of Deactivation Over Bimetallic Pt-Pd Catalysts with Different Pt Content

	Pt Content, w/w%											
	0.0	0.2	0.4	0.6	0.8	1.0	1.2	1.4	1.6	1.8	2.0	2.2
$\Delta\alpha/\alpha_{\text{ini}}, \%$ *	49	47	44	44	35	32	34	28	22	27	24	18

\*  $\Delta\alpha$ : decrease of conversion,  $\alpha_{\text{ini}}$ : initial conversion.

Catalyst loading: 100 mg; feed: 1% CH<sub>4</sub>, 10% O<sub>2</sub> and 89% He; flow rate: 50 mL/min; reaction temperature: 280 °C, data after 351 min TOS.

reduction at 350 °C in hydrogen (*reduced catalysts*), and (c) methane oxidation at 350 °C (*working catalysts*). All XP spectra were deconvoluted as described in the experimental part. The results of deconvolution of further XP spectra of mono- and multi-metallic catalysts are given in Tables 3-5.

### Pd 3d Core-Levels

The XP spectrum of the as prepared sample containing all three noble metals (Fig. 5A, spectrum "a") shows that in this sample the ionic form of palladium prevails. The reduction at 350 °C in hydrogen (see spectrum "b") resulted in a notable shift into the lower energy region, which is an indication on the partial reduction of palladium. The sample after methane oxidation (see spectrum "c") shows partial restoration of the oxidized forms; although the spectrum contains a well expressed shoulder around 335 eV. The latter might be an indication on the presence of some metallic palladium in the working Pt-Pd-Au/CeO<sub>2</sub> catalyst.

In Pd 3d core-level region three different Pd species were supposed to exist [18-20]. For this reason all Pd 3d bands were deconvoluted into three bands. These results are presented in Tables 3-5. The 3d<sub>5/2</sub> peaks between 334.8-335.5

eV and between 336.5-337.2 eV have been assigned to metallic Pd and PdO, respectively. Binding energies between 337.9-338.4 eV are significantly higher than that usually reported for PdO, implying the presence of Pd<sup>2+</sup> ions that are much more cationic than PdO. Pd<sup>2+</sup> species with highly cationic character could be present as Pd-O-Ce configuration [18-20].

### Pt 4f Core-Levels

The XP spectra given in Fig. 5B show the presence of both metallic and ionic forms of Pt in the sample containing all three noble metals. In the as prepared catalyst the platinum is fully oxidized, as no bands appear around 71.0 eV. However, as it has been expected the metallic character is well expressed in sample "b" after reduction at 350 °C in hydrogen. The XPS spectrum of working catalyst (see spectrum "c") shows that under condition of methane oxidation a relatively large part of platinum is still in metallic state. In Pt 4f core level region three species were also distinguished. According to different authors they can be assigned to Pt<sup>0</sup> (70.8-71.3 eV), Pt<sup>2+</sup> (72.4-72.9 eV), and Pt<sup>4+</sup> (73.9-74.4 eV), respectively [21, 22]. For this reason all Pt 4f bands were deconvoluted into three bands, attributed to the presence of

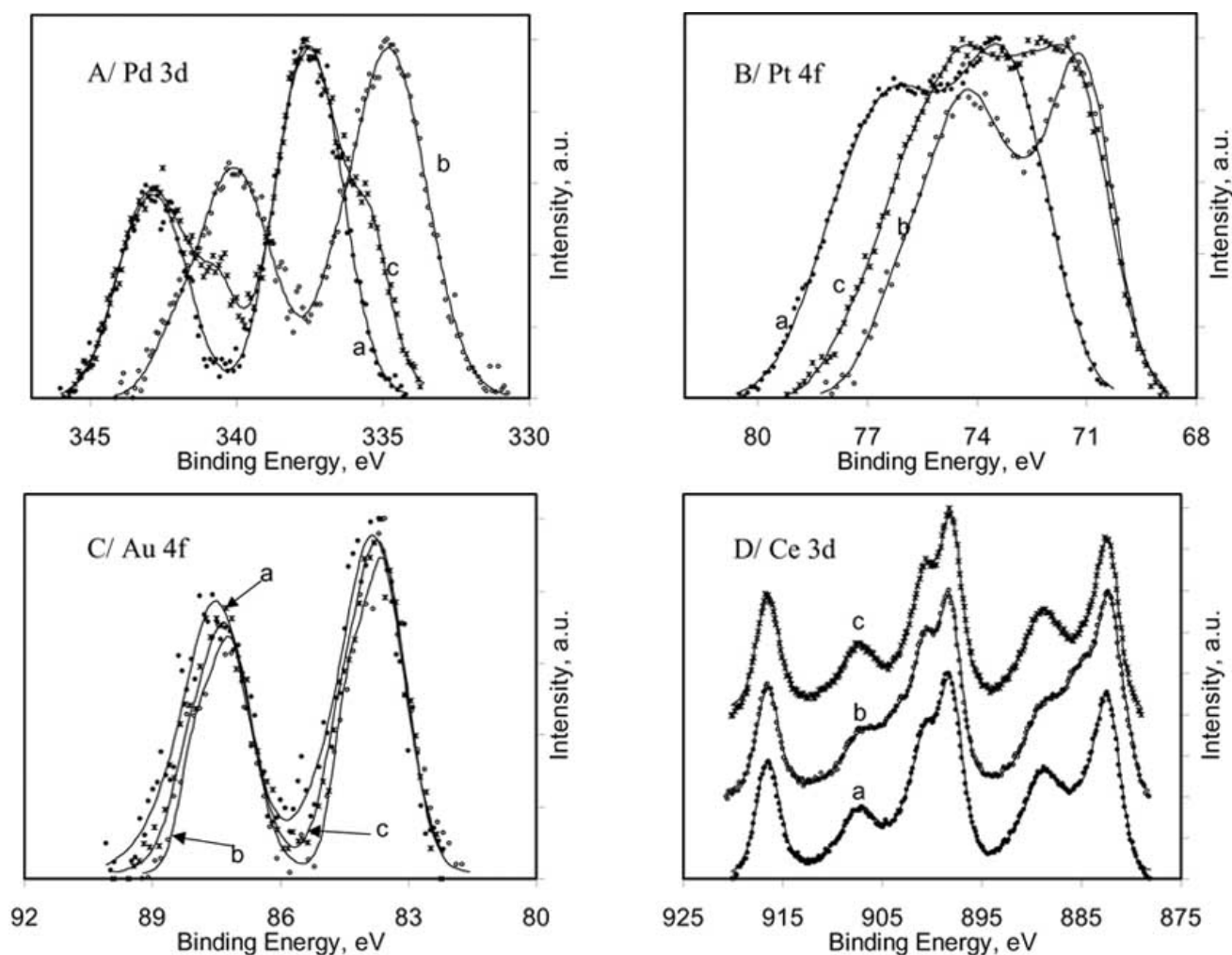


**Fig. (5).** X-ray photoelectron spectra of Pd 3d, Pt 4f, Au 4f and Ce 3d core level region (A, B, C and D) for catalyst 2%Pt-3%Pd-0.4%Au/CeO<sub>2</sub>; (a) before treatments, (b) after reduction in hydrogen at 350 °C, (c) working catalysts.

metallic Pt, PtO and PtO<sub>2</sub>. These results are presented in Tables 3-5.

#### Au 4f Core-Levels

The Au 4f spectra of the sample containing all three noble metals show only minor alterations after different pretreatment procedures (Fig. 5C). There is a very slight shift to the lower binding energy areas after reduction at 350 °C (see spectrum "b"). The working catalyst (see spectrum "c") has a slight shoulder at the high-energy site of the band. Consequently, the formation of ionic forms of gold is not excluded. It has to be mentioned however, that relatively small amount of Au (0.4%) was present, which gave rise to quite noisy spectra, analyses of which are relatively difficult. Therefore, these spectra were not deconvoluted.

#### Ce 3d Core-Levels

Fig. 5D shows the XPS results of the sample containing all three noble metals in the Ce 3d band region. The results show that the shape of Ce 3d spectrum after reduction in hydrogen at 350 °C (spectrum "b") differs from spectra both of as prepared sample (spectrum "a") and sample submitted to methane oxidation (sample "c"). Upon hydrogen treatment the intensities of component peaks, that indicate the reduction of ceria, have been enhanced. This is reflected in the shape of the spectra (compare spectra "b" and "a" in Fig. 5D). The reduction of ceria in the presence of noble metals is a well-known phenomenon. Noble metals like Pd have been reported to promote the oxygen mobility in ceria and reduction of Ce<sup>4+</sup> occurs due to the interaction with Pd [23]. The spectra "a" and "c" resemble to that of fully oxidized ceria [24]. Values of Ce<sup>3+</sup> concentration were calculated according to the method described in ref. [24]. The Ce 3d spectra were deconvoluted into 5 doublets according to ref. [24].

#### The Influence of Pretreatment Procedures

As it was demonstrated in Fig. 5, both in Pd 3d and Pt 4f regions the position of XP spectra can be used as the most straightforward way for comparison of oxidation states after different pretreatment process. Nevertheless, all spectra were also deconvoluted presuming different species. The surface concentrations of these species were calculated according to the intensities of different component peaks. Surface concentrations of different species, based on the deconvolution using spectral parameters described earlier, are summarized in Tables 3-5. These results provided further information about the role of Pt and Au on the stabilization of Pd in different valence state. XPS data of as prepared samples are collected

in Table 3, while data after hydrogen pretreatment and methane oxidation reaction are shown in Tables 4,5, respectively. Data given in Table 3 clearly indicate that in the as prepared form none of the samples contain metallic Pd. However, the introduction of Pt in 2 wt% strongly alters the PdO/ionic Pd(II) ratio, while this ratio is only slightly affected by the addition of gold.

As emerges from Table 4, the reductive treatment has a remarkable effect on the surface concentration of different species in the catalysts investigated. Addition of small amount of Pt already influences the PdO/ionic Pd(II) ratio. Further increase of the Pt content drastically changes the surface composition increasing the ratio of metallic Pd more than twice. The addition of small amount of gold results in further stabilization of Pd in metallic form. In the tri-metallic catalyst after reductive treatment Pd is almost in fully reduced state, as the doublet has been shifted significantly to lower binding energies with respect to spectrum obtained over the as prepared sample (compare spectra "b" and "a" in Fig. 5A). According to calculations, surface concentration of metallic Pd has reached a value as high as 95%. Data given in Table 4, clearly show that in case of catalyst 2%Pt-3%Pd-0.4%Au/CeO<sub>2</sub>, after reductive treatment the Pd is almost fully reduced, only 5% PdO can be calculated and there is no ionic Pd(II) formed in the sample.

In addition, changes in the oxidation state of Ce can also be followed by data given in Table 4. It is remarkable that on the monometallic catalyst the ceria support is reduced in a great extent. According to the calculations about half of the Ce<sup>4+</sup> is converted into Ce<sup>3+</sup>. However, in case of tri-metallic catalyst only 29% of the ceria is reduced after hydrogen treatment.

With respect to the interaction between Pd<sup>0</sup> and Ce<sup>4+</sup> we can refer to recent results [18]. Even if Pd is fully reduced to Pd<sup>0</sup> by hydrogen, the activated oxygen spillover from CeO<sub>2</sub> re-oxidizes Pd<sup>0</sup> to PdO while ceria is reduced to Ce<sup>3+</sup>. Doping of palladium, for example with rare earth metals, such as Pr or Gd, influences the extent of reduction of ceria support [18]. Therefore, the addition of other modifiers such as Pt and Au might also affect the reducibility of ceria.

This idea is in good accordance with our results. As emerges from Table 4, in the monometallic Pd catalyst the palladium can only be reduced partially, i.e. the relative concentration of Pd<sup>0</sup> is only 28%, while the amount of ionic Pd (II) is relatively high (16%). Simultaneously, over the monometallic catalyst the ceria support is reduced in a great

**Table 3. XPS Data of as Prepared Samples**

Catalysts	Pd Species <sup>1</sup> (%)			Pt Species <sup>2</sup> (%)			Ce(III) <sup>3</sup>
	Pd	PdO	Ionic Pd(II)	Pt	PtO	PtO <sub>2</sub>	
3%Pd/CeO <sub>2</sub>	0	25	75	-	-	-	10
1%Pt-3%Pd/CeO <sub>2</sub>	0	33	67	0	43	57	10
2%Pt-3%Pd/CeO <sub>2</sub>	0	66	34	5	51	44	6
2%Pt-3%Pd-0.4% Au/CeO <sub>2</sub>	0	60	40	0	37	63	8

<sup>1</sup>Pd (334.8-335.5 eV), PdO (336.5-337.2 eV) and ionic Pd(II) (337.9-338.4 eV) have been involved into the deconvolution process.

<sup>2</sup>Pt (70.8-71.3 eV), PtO (72.4-72.9 eV) and PtO<sub>2</sub> (73.9-74.4 eV) have been involved into the deconvolution process.

<sup>3</sup>Concentration of Ce<sup>3+</sup>.

**Table 4.** XPS Data After Pretreatment in Hydrogen at 350 °C

Catalysts	Pd Species (%)			Pt Species (%)			Ce(III)
	Pd	PdO	Ionic Pd(II)	Pt	PtO	PtO <sub>2</sub>	
3%Pd/CeO <sub>2</sub>	28	56	16	-	-	-	51
1%Pt-3%Pd/CeO <sub>2</sub>	29	64	7	35	50	15	49
2%Pt-3%Pd/CeO <sub>2</sub>	68	32	0	69	31	0	29
2%Pt-3%Pd-0.4% Au/CeO <sub>2</sub>	95	5	0	62	38	0	29

For spectral parameters see Table 3.

extent (50%). In case of multi-metallic catalysts the opposite trends were obtained, i.e. reduction of Pd is favored to that of ceria. In catalyst 2%Pt-3%Pd-0.4% Au/CeO<sub>2</sub> the Pd is in metallic form in 95%, while only 29% of the ceria is reduced after hydrogen treatment. The results unambiguously indicate that both Pt and Au facilitate the reduction of Pd and prevent the re-oxidation of Pd by the ceria support. Consequently, both platinum and gold have a very pronounced influence on the stabilization of Pd in metallic form on the ceria support. However, data given in Table 4 also indicate that gold has almost no influence on the surface concentration of different forms of Pt and the amount of Ce(III) formed.

The analysis of data given in Table 5 gives further explanation on the role of Pt in the bi- and tri-metallic catalysts. In the bi- and tri-metallic catalysts after methane oxidation Pd is present in more reduced state than in the monometallic catalyst. These results indicate that over multi-metallic catalysts after methane oxidation metallic Pd can still be detected in the amount of 20%, i.e. Pd remains partly in a reduced state even under conditions of methane oxidation. In catalysts with high Pt content the fraction of ionic Pd(II) species is relatively low, its ratio is around 30%.

These results also indicate that both Pt and Pd metals remained at least partly in reduced state even after submission to oxidative reaction conditions. It is especially surprising in case of Pd, as PdO forms between ca. 300–400 °C, being stable in air at atmospheric pressure up to 800 °C [25].

The stabilization effect of Pt is well documented in Fig. 6, which shows the XPS spectra of Pd 3d core level after methane oxidation over various catalysts containing different amount of Pt. The doublets in the Pd 3d spectra of bi- and tri-metallic catalysts have a shoulder at the low binding energy side (spectra “b” and “c”, respectively), whereas the spectrum of the monometallic Pd catalyst (spectrum “a”) consists of a well resolved doublet shifted towards the high binding energy regions indicating higher oxidation state of Pd in this system as compared to multi-metallic catalysts.

In addition, it has to be emphasized that according to data given in Table 5 the formation of ionic Pd(II) is strongly hindered in the catalysts containing at least 2% Pt. We consider that the ionic Pd(II) form in the catalysts is not involved either in the methane activation or in the oxidation step. Consequently, the decrease of the ionic Pd(II) content in the working catalyst is a very important issue to control the activity of methane oxidation over Pd/CeO<sub>2</sub> catalysts.

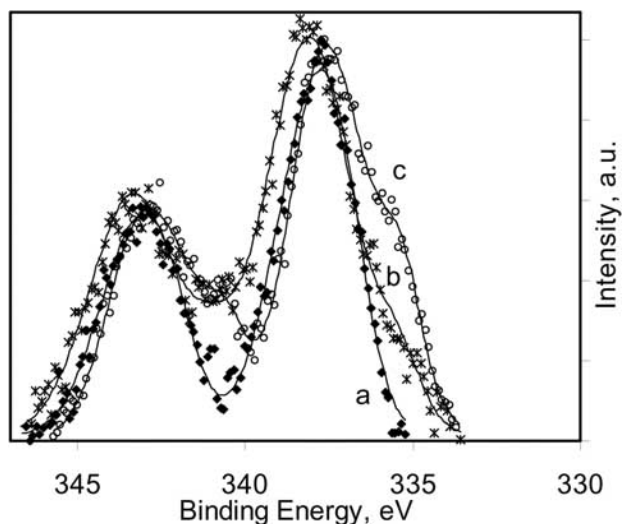


**Fig. (6).** X-ray photoelectron spectra of Pd 3d core level region for working catalysts: (a) 3%Pd/CeO<sub>2</sub>, (b) 1%Pt-3%Pd/CeO<sub>2</sub>, (c) 2%Pt-3%Pd-0.4% Au/CeO<sub>2</sub>.

In summary the good agreement between the XPS and the catalytic data has to be emphasized. Based on results of our activity tests the presence of partially reduced surface Pd species has been predicted over the working multi-metallic catalysts. This suggestion has been supported by our XPS results. The higher activation energies obtained on multi-metallic catalysts were attributed to the presence of metallic Pd on the surface, which has also been evidenced by the XPS analysis.

Additionally, in our catalytic system two different types of Pd(II) have been identified by XPS. Upon addition of Pt and Au the amount of the first type (PdO like species) at lower binding energies increases, while the amount of the second type (Pd(II) with more expressed ionic character) detected at higher binding energies, decreases (Table 5).

The correlation of T<sub>90</sub> data (Table 1) with XPS results given in Table 5 shows that in the activity control the coexistence of the PdO and metallic Pd is crucial. The less of the amount of ionic Pd(II) form in a given catalyst the higher the catalytic activity in methane oxidation. It is suggested that the surface ionic Pd(II) form is isolated from the surface metallic Pd and thought to be much less active than the boundary contact between metallic Pd and PdO, i.e., the Pd<sup>0</sup>–PdO ensemble sites.

Table 5. XPS Data Over Working Catalysts

Catalyst	Pd Species (%)			Pt Species (%)			Ce(III)
	Pd	PdO	Ionic Pd(II)	Pt	PtO	PtO <sub>2</sub>	
3%Pd/CeO <sub>2</sub>	0	21	79	-	-	-	10
1%Pt-3%Pd/CeO <sub>2</sub>	11	14	75	25	41	34	8
2%Pt-3%Pd/CeO <sub>2</sub>	22	48	30	62	29	8	5
2%Pt-3%Pd-0.4% Au/CeO <sub>2</sub>	20	50	30	57	32	11	7

For spectral parameters see Table 3.

Based on XPS data the deactivation features can also be interpreted. The surface composition right after the hydrogen pretreatment might be associated with the initial activity, whereas the stable activity is supposed to be controlled by the surface composition formed during methane oxidation. The working catalyst should have Pd-PdO interaction to maintain its high activity. The loss of either the metallic Pd or the PdO like species would result in a loss of activity.

According to our assumption the steady-state activity should correlate with the number of Pd<sup>0</sup>-PdO ensemble sites formed in situ. As emerges from Table 5, these sites are either missing or are in very low concentration over the monometallic Pd catalyst. The introduction of Pt increases the chance for the formation of Pd<sup>0</sup>-PdO ensemble sites and their optimum concentration can be achieved when the Pt content is around 2 wt%.

### Characterizations by FTIR Spectroscopy of CO Chemisorption

CO adsorption at room temperature on monometallic Pd-catalyst resulted in the FTIR spectra shown in Fig. 7A. When all adsorption sites are saturated (spectrum "a"), the main band, in the region characteristic for carbonyl adsorption, is centered at 2064 cm<sup>-1</sup>, which can be assigned to linearly adsorbed carbonyl species on reduced Pd<sup>0</sup>, whereas the band at 1954 cm<sup>-1</sup> should be attributed to bridged carbonyl species. These bands appear at slightly lower frequencies than it is

published in the related art on Pd catalysts supported on SiO<sub>2</sub> and/or Al<sub>2</sub>O<sub>3</sub> [26]. This small difference might be due to the interaction of Pd particles with ceria support as described elsewhere [27]. The decrease in the particle size can also account for the slight decrease in the wave numbers [28]. Additionally, the particle size correlates with the ratio of peak areas of the linear to bridged carbonyl signals as well [29]. The larger this ratio the smaller is the particle size of the supported nanocluster. It has to be mentioned that in spectra given in Fig. 7A the ratio of linear to bridged carbonyl signals is much higher than that in spectra shown in refs. [26,29]. Accordingly, the degree of agglomeration of Pd particles in catalysts investigated in this study might be lower than in refs. [26,29], which in turn might account for the lower frequency of linearly adsorbed carbon monoxide.

After degassing the sample at room temperature (Fig. 7A, spectrum "b") there is a remarkable decrease in the intensity of the high frequency band, together with a pronounced shift toward lower frequencies (2021 cm<sup>-1</sup>). This observation can be attributed to the decrease of dipole-dipole interaction between adjacent CO molecules at decreasing coverage. The band assigned to bridged carbonyl species remains almost unchanged after evacuation. The four supplementary bands below the region of the carbonyl adsorption (at 1577, 1557, 1364 and 1337 cm<sup>-1</sup>) correspond to the formation of carbonate and formate species on CeO<sub>2</sub> [26]. The intensities of these bands increase even after evacuation (compare spectrum "b" to "a").

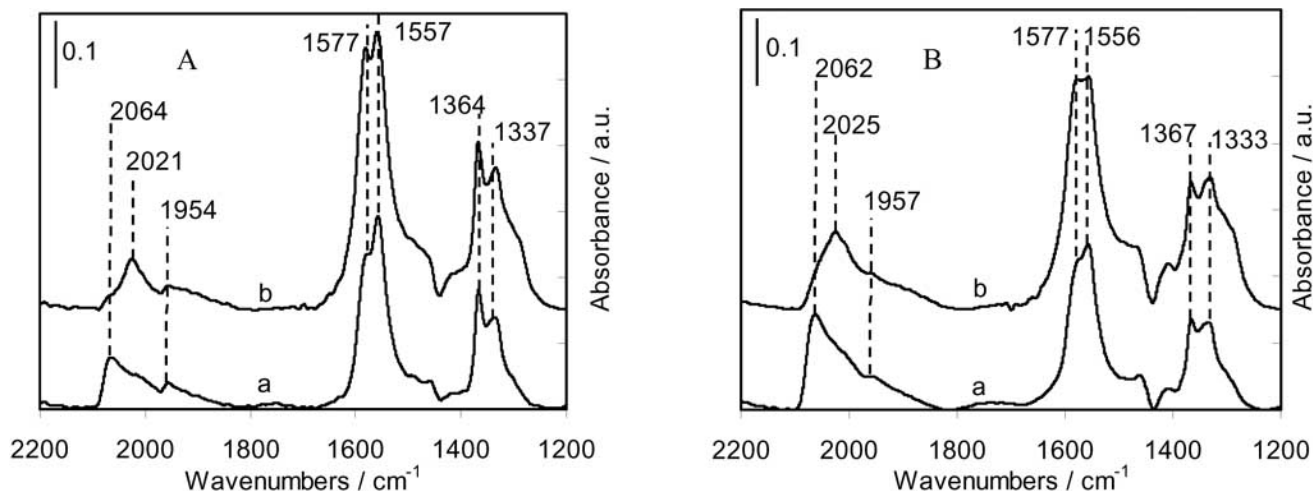


Fig. (7). FTIR spectra of CO adsorbed on catalysts 3%Pd/CeO<sub>2</sub> and 2%Pt-3%Pd/CeO<sub>2</sub> (A and B) after hydrogen treatment at 400 °C. Spectra were taken; (a) in the presence of 5 mbar CO and (b) after degassing at room temperature.

Surprisingly, no significant changes in the positions of corresponding bands were observed when a bimetallic catalyst (2%Pt-3%Pd/CeO<sub>2</sub>) was investigated (Fig. 7B). Practically, the spectra show characteristic features obtained over monometallic Pd catalyst. Although, the stretching vibration of linearly adsorbed Pt-CO carbonyl species over a monometallic Pt catalyst can be situated at the same position as over a monometallic Pd catalyst, the absorption assigned to bridged Pt<sub>2</sub>-CO species should appear around 1840 cm<sup>-1</sup> in case of a supported monometallic Pt catalyst [31]. This latter band, however, is missing from the spectra given in Fig. 7B. Thus, spectra in Fig. 7B cannot be considered as simple superposition of spectra of two single metals Pt and Pd. Nevertheless, there is one remarkable difference between the spectra of adsorbed CO over the monometallic Pd/CeO<sub>2</sub> (Fig. 7A) and the bimetallic Pt-Pd/CeO<sub>2</sub> catalysts (Fig. 7B). Over the bimetallic catalyst the ratio of bridged Pd<sub>2</sub>-CO signal to linear Pd-CO signal decreased significantly compared to the monometallic catalyst. Eventually, the two effects, namely the lack of bridged Pt<sub>2</sub>-CO species and the reduction of bridged Pd<sub>2</sub>-CO species point to the dilution effect by Pt atoms. As a consequence, the amount of Pd-Pd and Pt-Pt bonds is decreased and replaced by Pd-Pt bond, which hinders the formation of bridged species. Based on these results it can be concluded that in the bimetallic catalyst there is an intimate contact between Pd and Pt, i.e. we have an indirect evidence for the formation of Pd-Pt alloys in the bimetallic catalyst.

It is also remarkable that in the FTIR spectra the intensity of carbonyl bands is higher over the bimetallic than over the monometallic Pd catalyst (compare Fig. 7A and 7B). Of course, it is partly due to the higher noble metal content of the bimetallic system, but the effect of a possible higher metal dispersion in the bimetallic catalyst cannot be excluded. This assumption is supported by data given in Table 6. As emerges from these data the ratio of the amount of adsorbed CO to the total noble metal content increased significantly in case of bi- and tri-metallic catalysts in comparison to monometallic Pd one. Accordingly, the addition of Pt and Au increase the metal dispersion in multi-metallic catalysts, which partly can be responsible for the more intensive carbonyl bands in FTIR spectra over these catalysts. Eventually, the higher exposed metallic area shows good correlation with the higher methane oxidation activity of multi-metallic catalysts compared to the monometallic one.

**Table 6. Results of CO Chemisorption on Different Catalysts**

Catalysts	CO <sub>ads</sub> /(Pt+Pd+Au) <sup>1</sup>
	mol/at
3%Pd/CeO <sub>2</sub>	0.30
1%Pt-3%Pd/CeO <sub>2</sub>	0.39
2%Pt-3%Pd/CeO <sub>2</sub>	0.41
2%Pt-3%Pd-0.4%Au/CeO <sub>2</sub>	0.37

<sup>1</sup>Ratio of adsorbed amount of CO to total noble metal content.

### Temperature Programmed Desorption of Hydrogen (TPD)

The alloy formation in mixed metal catalysts was also confirmed by hydrogen TPD. The corresponding hydrogen

desorption curves are shown in Fig. 8. Based on literature, desorption data at low temperature, i.e. below 120 °C, depicts the decomposition of β-PdH<sub>x</sub>, where x=0.76 [32]. As emerges from Fig. 8 the amount of hydrogen evolved at this temperature is significantly lower over multi-metallic catalysts than over the monometallic Pd one. It means that the monometallic Pd catalyst has higher affinity for hydride formation, whereas the hydride formation is hindered on bi- and trimetallic catalysts. The addition of Pt and Au to palladium inhibits the formation of β-PdH<sub>x</sub> most probably because of alloying Pd with Pt.

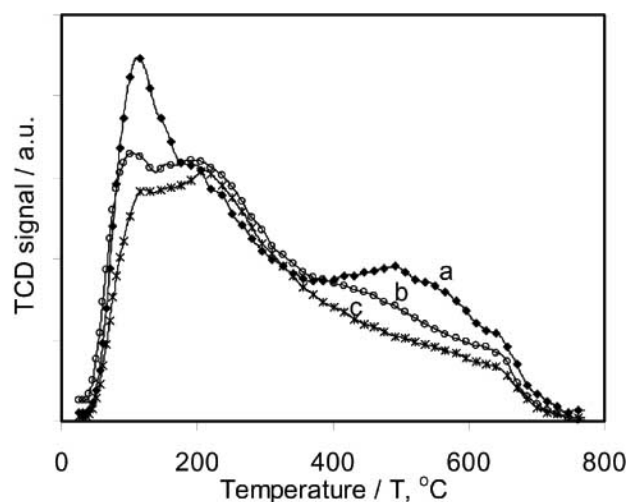


**Fig. (8).** Temperature programmed desorption of hydrogen on catalysts; (a) 3%Pd/CeO<sub>2</sub>, (b) 2%Pt-3%Pd/CeO<sub>2</sub>, and (c) 2%Pt-3%Pd-0.4%Au/CeO<sub>2</sub> after hydrogen treatment at 350 °C.

The origin of the hydrogen desorbed at higher temperatures on different catalysts has not been fully understood yet. Ceria support might have lattice defects that serve as acceptors for storage of hydrogen species. It is supposed that hydrogen species that adsorbed on Pd or Pt can spill over to ceria support on which they are stored in lattice defects. It is remarkable that the higher the Pt and Au content the less the amount of the desorbed hydrogen at elevated temperature (above 400 °C). The monometallic Pd catalyst is considered to be more active in spillover of hydrogen than the bi- and trimetallic systems.

### SUMMARY

One of the goals in this paper was the verification of the use of high-throughput experimentation in academic, basic research. Catalysts have been prepared and tested by using high-throughput equipment and methods. During catalyst library design our research strategy was to find the best compositions in a multi-dimensional experimental space as fast as possible [12]. Accordingly, ceria supported mixed metal catalysts containing Pt, Pd and Au had been found to have the highest activity on methane total oxidation at 350 °C. As a continuation of the previous work in the present study these tri-metallic catalysts were investigated and the role of Pt and Au has been elucidated. It has been shown that the addition of Pt and Au to palladium promotes the methane oxidation activity as well as improves the long-term stability compared to the monometallic Pd catalyst. The formation of

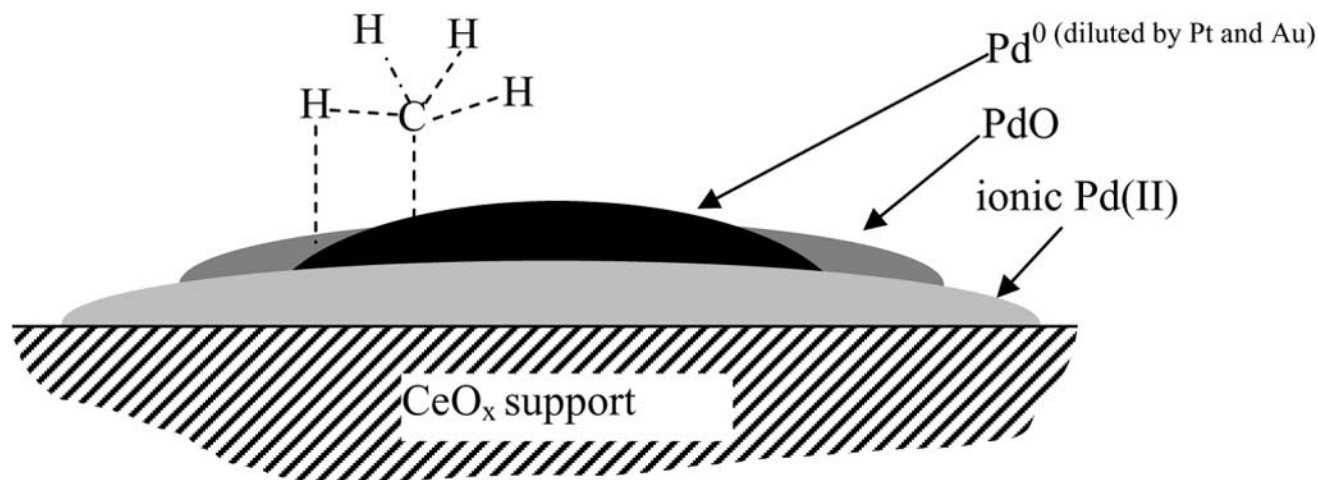


Fig. (9). Scheme of methane activation over Pd<sup>0</sup>-PdO ensemble sites.

new active sites has been supposed which adsorb methane stronger than in the monometallic Pd catalyst.

In multi-metallic catalysts containing both Pt and Pd the oxidation state of active species after different pretreatment including methane oxidation has been investigated. It has been shown that coexistence of both metallic Pd<sup>0</sup> and PdO is required to get highly active catalysts. We suggest that the activation of methane takes place over Pd<sup>0</sup> – PdO ensemble site, as shown in Fig. 9, presenting a cross-section of a trimetallic particle supported on CeO<sub>2</sub>. Similar mechanistic view was suggested in earlier studies [5,6]. Of course, in our system Pd<sup>0</sup> represents the tri-metallic system, in which Pd is diluted by Pt and Au.

It was also shown that in highly active catalysts the amount of the third form of palladium, i.e. ionic Pd(II), is strongly reduced on the surface. However, the results indicate that this form of Pd is not involved in the catalytic process. This species can be considered as “spectator” in the methane oxidation (Fig. 9).

The high activity of multi-metallic catalysts was attributed to the formation of Pd<sup>0</sup> – PdO ensemble sites. Contrary to this, the monometallic Pd catalyst after methane oxidation contained no metallic Pd and the formation of ionic Pd(II) type species prevailed over PdO. In multi-metallic catalysts beside the formation of the new type of active sites the exposed metallic surface has also been increased that also shows good correlation with the increased activity. The advantageous effect of Pt and Au on the catalytic activity of Pd-based ceria supported catalysts is, most probably, due to the intimate contact between three noble metals.

It is known that Pt alone is not an active catalyst for low temperature methane activation. Consequently, the addition of Pt to Pd has an indirect influence in the activity control, namely it strongly alters the ratio between different forms of palladium. The XPS results provided unambiguous evidence that the addition of Pt to Pd decreases the amount of catalytically inactive ionic type Pd (II) species.

In all multi-metallic catalysts indirect evidences were found for alloying of Pt with Pd. It can finally be concluded that the improved catalytic properties of multi-metallic Pt-Au-Pd/CeO<sub>2</sub> catalysts to the monometallic Pd one are due to (i) the increase of the number of Pd<sup>0</sup> – PdO dual-type active

sites, (ii) stronger methane adsorption on the Pd<sup>0</sup> – PdO boundary, (iii) higher accessible metallic area in the working catalyst, and (iv) suppression of the reduction of Ce (IV) in the presence of Pt.

#### ACKNOWLEDGEMENTS

Partial financial support given to A.T. (OTKA grant N° F 049742) is greatly acknowledged. The CSIC-HAS bilateral agreement is also acknowledged.

#### REFERENCES

- [1] Sekizawa, K.; Machida, M.; Eguchi, K.; Arai, H. *J. Catal.*, **1993**, *142*, 655.
- [2] Burch, R.; Urbano, F.J. *Appl. Catal. A: Gen.*, **1995**, *124*, 121.
- [3] Lyubovskiy, M.; Pfefferle, L. *Appl. Catal. A: Gen.*, **1998**, *173*, 107.
- [4] Datye, A.K.; Bravo, J.; Nelson, T.R.; Atanasova, P.; Lyubovskiy, M.; Pfefferle, L. *Appl. Catal. A: Gen.*, **2000**, *198*, 176.
- [5] Su, S.C.; Carsten, J.N.; Bell, A.T. *J. Catal.*, **1998**, *176*, 125.
- [6] Lin, W.; Zhu, Y.X.; Wu, N.Z.; Xie, Y.C.; Murwani, I.; Kemnitz, E. *Appl. Catal. B: Environ.*, **2004**, *50*, 59.
- [7] Groppi, G.; Artioli, G.; Cristiani, C.; Lietti, L.; Forzatti, P. *In Studies in Surface Science and Catalysis*; E. Iglesia et al., Eds.; Elsevier: Amsterdam, **2001**; Vol. *136*, pp. 345.
- [8] Arai, H.; Machida, M. *Catal. Today*, **1991**, *10*, 81.
- [9] Roth, D.; Gelin, P.; Primet, M.; Tena, E. *Appl. Catal. A: Gen.*, **2000**, *203*, 37.
- [10] Hoyos, L.J.; Praliaud, H.; Primet, M. *Appl. Catal. A: Gen.*, **1993**, *98*, 125.
- [11] Narui, K.; Yata, H.; Furuta, K.; Nishida, A.; Kohtoku, Y.; Matsuzaki, T. *Appl. Catal. A: Gen.*, **1999**, *179*, 165.
- [12] Tompos, A.; Margitfalvi, J.L.; Tfirst, E.; Végvári, L.; Jaloull, M.A.; Khalfalla, H.A.; Elgarni, N.M. *Appl. Catal. A: Gen.*, **2005**, *285*, 65.
- [13] Janbey, A.; Clark, W.; Noordally, E.; Grimes, S.; Tahir, S. *Chemosphere*, **2003**, *52*, 1041.
- [14] Hoffmann, C.; Wolf, A.; Schüth, F. *Angew. Chem.-Int. Ed.*, **1999**, *38*, 2800.
- [15] Hilaire, S.; Wang, X.; Luo, T.; Gorte, R.J.; Wagner, J.P. *Appl. Catal. A: Gen.*, **2001**, *215*, 271.
- [16] Sharma, S.; Hilaire, S.; Vohs, J.M.; Gorte, R.J.; Jen, H.-W. *J. Catal.*, **2000**, *190*, 199.
- [17] Wang, X.; Gorte, R.J.; Wagner, J.P. *J. Catal.*, **2002**, *212*, 225.
- [18] Borchert, H.; Borchert, Y.; Kaichev, V.V.; Prosvirin, I.P.; Alikina, G.M.; Lukashevich, A.I.; Zaikovskii, V.I.; Moroz, E.M.; Paukshtis, E.A.; Bukhtiyarov, V.I.; Sadikov, V.V. *J. Phys. Chem. B*, **2005**, *109*, 20077.
- [19] Sun, K.; Lu, W.; Wang, M.; Xu, X. *Appl. Catal. A: Gen.*, **2004**, *268*, 107.
- [20] Xiao, L.; Sun, K.; Xu, X.; Li, X. *Catal. Commun.*, **2005**, *6*, 796.
- [21] Tang, X.; Zhang, B.; Li, Y.; Xu, Y.; Xin, Q.; Shen, W. *J. Mol. Catal. A: Chem.*, **2005**, *235*, 122.

- [22] Shyu, J.Z.; Otto, K. *Appl. Surf. Sci.*, **1998**, *32*, 246.
- [23] Kepinski, L.; Okal, J. *J. Catal.*, **2000**, *192*, 48.
- [24] Zhang, F.; Wang, P.; Coberstein, J.; Khalid, S.; Chan, S.-W. *Surf. Sci.*, **2004**, *563*, 74.
- [25] Farrauto, R.J.; Lampert, J.K.; Hobson, M.C.; Waterman, E.M. *Appl. Catal. B: Environ.*, **1995**, *6*, 263.
- [26] Pawelec, B.; Parola, V.L.; Thomas, S.; Fierro, J.L.G. *J. Mol. Catal. A: Chem.*, **2006**, *253*, 30.
- [27] Bensalem, A.; Bozon-Verduraz, F.; Delamar, M.; Bugli, G. *Appl. Catal. A: Gen.*, **1995**, *121*, 81.
- [28] Kappers, M.J.; van der Maas, J.H. *Catal. Lett.*, **1991**, *10*, 365.
- [29] Craciun, R.; Daniell, W.; Knözinger, H. *Appl. Catal. A: Gen.*, **2002**, *230*, 153.
- [30] Lavalley, J.-C.; Saussey, J.; Lamotte, J.; Breault, R.; Hindermann, J.P.; Kiennemann, A. *J. Phys. Chem.*, **1990**, *94*, 5941.
- [31] Albertazzi, S.; Busca, G.; Finocchio, E.; Glöckler, R.; Vaccari, A. *J. Catal.*, **2004**, *223*, 372.
- [32] Ozkan, U.S.; Kumthekar, M.W.; Karakas, G. *Catal. Today*, **1998**, *40*, 3.

---

Received: October 15, 2006

Revised: November 19, 2006

Accepted: November 20, 2006